Detection and Identification of Converted Modes and Shallow Structure Mapping in the Groningen Gas Field

Ali Fuad AlJishi, Oleg V. Poliannikov and Michael C. Fehler, Earth Resources Laboratory, Massachusetts Institute of Technology*

SUMMARY

Passive seismic monitoring waveform data collected at the Groningen gas field contain many interesting events besides direct P- and S-arrivals. We examine some of these arrivals in order to understand their nature. A combination of move-out analysis, ray-tracing and finite-difference simulations has revealed that the data contain converted phases from two shallow interfaces. By using a kinematic version of the Source Independent Converted Phase Imaging Condition, we can map those interfaces.

INTRODUCTION

The Groningen gas field is located in the Groningen province of the Netherlands. It has been producing large volumes of gas since 1963. Earthquakes, thought to be primarily induced by compaction, have been observed in the area since 1986. In response, a larger array was installed to collect and analyze seismic data.

The recorded data are quite complex, largely due to the complex geology of the area. In particular, there is a large salt body and two layers of extremely fast anhydrites, while the velocities at shallow depths are very low due to unconsolidated materials. As a result, seismic waves travel through a complicated velocity model with large contrasts, and many hard-to-identify phases, in addition to direct arrivals, are observed for most earthquakes. Instead of being a nuisance, these phases present an opportunity to glean more information about the subsurface surrounding the reservoir.

We analyze data recorded by several stations and look at various phases generated by earthquakes. We use finite-difference modeling and kinematic analysis to identify them. We show that the data contain at least two *s-to-p* conversions and one *p-to-s* conversion.

Shabelansky et al. (2015) have developed the Source Independent Converted Phase Imaging Condition that uses phase conversions at an interface to image that interface. We use a simplified kinematic form of that method to image structures that give rise to the conversion we see in the Groningen data. A comparison of our results to the velocity model provided by the operator reveals a close match for most stations.

IDENTIFICATION OF CONVERTED PHASES

Figure 1 shows seismic event data recorded at G45 borehole for a waveform on February 25, 2016. Each trace corresponds to a different level inside the borehole. The data appear fairly complex showing many different phases. For illustration purposes, we show only the vertical component waveforms at one borehole, but all components at many more boreholes were used in our analysis.

Looking at Figure 1, we see a P-wave that arrives first around 1 s, and an S-wave that arrives around 3 s. The relative amplitude of the S-wave is much larger on the horizontal components. Both P- and S-waves are reflected from the surface, and the reflection is also recorded as manifested by events with the opposite slopes.

In addition to the direct arrivals, we can clearly see at least two other phases that arrive later than the P-wave but earlier than the S-wave. These arrivals are indicated in Figure 1 by red arrows. In addition, another phase appears right before the direct S-wave arrival. In order to see all events more clearly, we calculate moving window averages of the amplitudes of all three components recorded by the surface receiver, and show them in Figure 2. The converted phases indicated by the two red arrows and a green arrow stand out even more distinctly.

By comparing the move-out of these events to the move-outs of the direct P- and S-arrivals, we can see that the events marked with red arrows arrive as P-waves, and the phase marked with a green arrow arrives as an S-wave. Their amplitudes rule out the possibility that they are P-wave multiples. It therefore stands to reason to suspect that the first two are *s-to-p* conversions at some subsurface interface, and the last one is a *p-to-s* conversion.

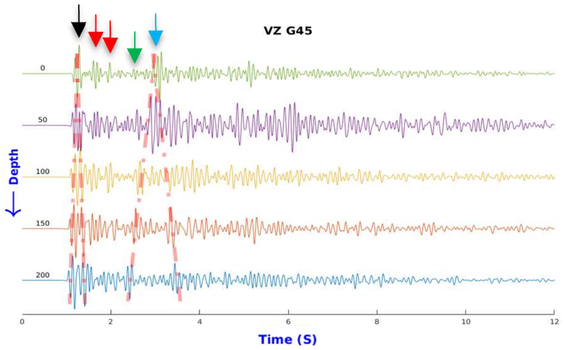

Figure 1 Vertical component seismic traces recorded in borehole G45 for the 25th of February 2016, magnitude 2.4 event. Receiver depths are marked next to each trace. Dashed lines indicate the direct P and S phases and their reflection form the surface. Arrows point to phases that are discussed in the text.

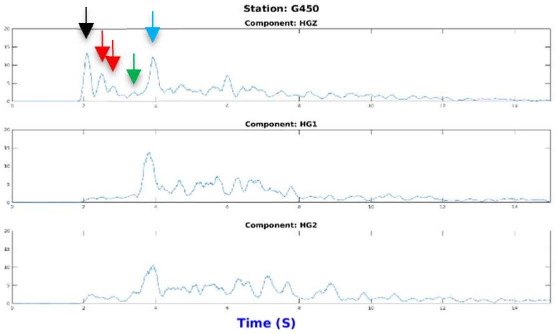

Figure 2 Smoothed trace amplitudes recorded at the surface of borehole G45. HGZ is the vertical component, HG1 is the north component and, HG2 is the east component. Arrows point to phases discussed in the text.

CONVERSION LOCATION BY WAVEFORM MODELING

The velocity/density model provided to us by the operator contains several interfaces. Versions of this model have been previously published in Kraaijpoel et al. (2013). In order to identify interfaces that correspond to each observed converted phase, we use a finite-difference forward solver to model waveforms that should be observed at different stations. We used catalog x and y-coordinates of the source, and adjusted the depth and origin time to fit direct arrivals. Figure 3 shows simulation results for the same station as the data shown before.

Identification of the origins of each phase is a semimanual process. We decompose the elastic wavefield into a P- and S-wavefields and observe the propagation of individual phases. We find that we are able to detect the location, time and interface at which phase conversions occur, and we also can track these conversions to the surface and record the times of their arrivals.

Upon completion of this intensive exercise, we are able to associate each *s-to-p* conversion shown in Figure 1 to a corresponding interface. We conclude that the two *s-to-p* modes present in the gathers are generated by the base of the North Sea supergroup unconformity and the base of the Chalk group unconformity (Wong et al., 2007).

Our results have been independently verified by ray-tracing of the same velocity model. We used a simplistic ray-tracer that effectively uses an S-wave velocity model up to a certain interface and a P-wave velocity model after that to calculate an *s-to-p* conversion travel time. However, relying just on the ray-tracer may be problematic because it is not obvious that high-frequency simulations give a good representation of how finite-frequency waves propagate in a velocity model as complicated as the Groningen velocity model.

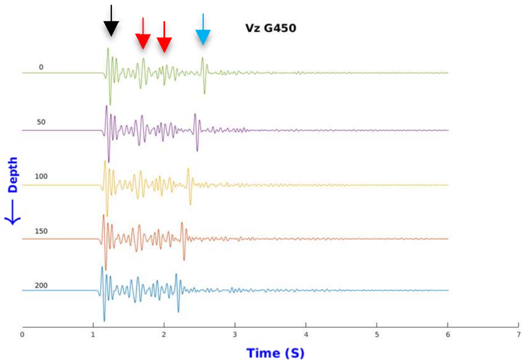

Figure 3 Vertical component of the elastic wave-field calculated using finite-difference modeling to mimic the data recorded in borehole G45.

We note that the traces shown in Figure 3 do not contain surface reflections because we used a PML boundary in our simulations. Also, the model predicts many more phases, mostly *p-to-s* conversions at different interfaces. These phases are hard to identify in field data. The fact that we do not account for attenuation and thus potentially overestimate amplitudes of some phases partially explains this phenomenon.

CONVERTED PHASE IMAGING

Shabelansky et al (2015) have proposed the Source Independent Converted Phase Imaging Condition for imaging structures using phase conversion caused by these structures. Their method requires a direct S-wave and an *s-to-p* conversion (or a direct P-wave and a *p-to-s* conversion) to map an interface. Imaging is accomplished by back-propagating each of the phases from the surface through the velocity model in the reverse direction of time. Because of how the two phases are naturally timed with respect to one another, they will refocus at the point of conversion. An important feature of this algorithm is that the location and the origin time of the source are irrelevant so long as these phases are properly labeled.

Because the S-wave and the *s-to-p* conversion (or the P-wave and the *p-to-s* conversion) do not propagate along the same path, a good receiver coverage is required in order to image using these phases. Here we use a simplified version of this algorithm by assuming near-vertical propagation above the conversion point, in which case simple kinematic shifts of traces are good approximations of back-propagation.

We use this simplified imaging method to create a map of the interfaces below many stations. For each station, we try to find events that have a clear direct S-wave arrival and the two *s-to-p* conversions discussed above. This is not an automated process because the signal quality of these phases depends on the proximity of the event, its magnitude, and source mechanism.

A strong event directly below the station would give us the desired vertical propagation path. Unfortunately, such events are not typically available for most stations. Therefore, we estimate the zero-offset arrival time by extrapolating the move-out obtained from arrivals of available events.

The kinematic imaging condition for Source Independent Converted Phase Imaging Condition is conceptually equivalent to locating a "source" located at the point of phase conversion (Aki & Richards, 2002). Once the *s-to-p* conversion occurs, this imaginary source "emits" S (direct S) and P (*s-to-p* conversion) waves that both propagate vertically. Denote with T the propagation time from the interface to the surface in the P-wave velocity model. Then we have

$$(t_s - t_{sp})v_s + Tv_s = Tv_p \tag{1}$$

where t_s is the arrival time of the direct shear wave at the zero offset, t_{sp} is the arrival time of the *s*-to-*p* conversion mode at zero offset, and both sides equal the depth of the interface. Solving for T, we obtain

$$T = v_s \frac{t_s - t_{sp}}{v_p - v_s} \tag{2}$$

The depth of the interfaces at which the *s*-to-*p* conversion happens has the form:

$$z = v_p v_s \frac{t_s - t_{sp}}{v_p - v_s} \tag{3}$$

Analysis of *p-to-s* conversions can be done similarly. The depth of an interface that generates a *p-to-s* conversion is given by:

$$z = v_p v_s \frac{t_{ps} - t_p}{v_p - v_s} \tag{4}$$

where t_p is the arrival time of the direct compressional wave at the zero offset, t_{ps} is the arrival time of the *p*-to-*s* conversion at zero offset.

The velocities used in the preceding calculations, v_p and v_s, are taken as the harmonic mean of the compressional and shear velocity between the interface and the station, which corresponds to averaging the slownesses.

We calculate the interface depths according to Equation 3 for various stations and construct 2D surfaces of the two structures, the base of the North Sea supergroup unconformity and the base of the Chalk group unconformity, that correspond to the two *s-to-p* conversions previously identified. Their contour plots are shown in Figures 4 and 5 respectively.

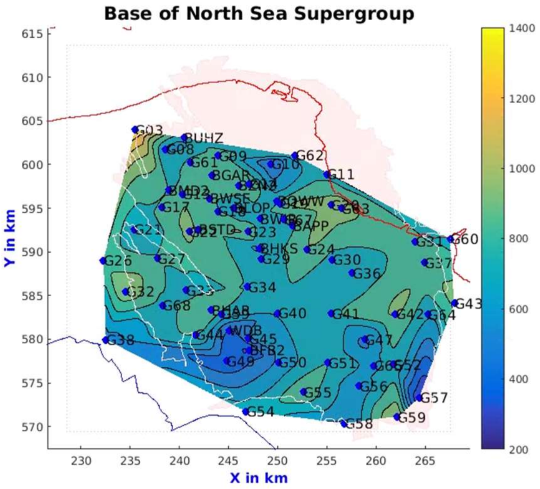

Figure 4 The depth calculated using equation (3) for the base of the North Sea surpergroup.

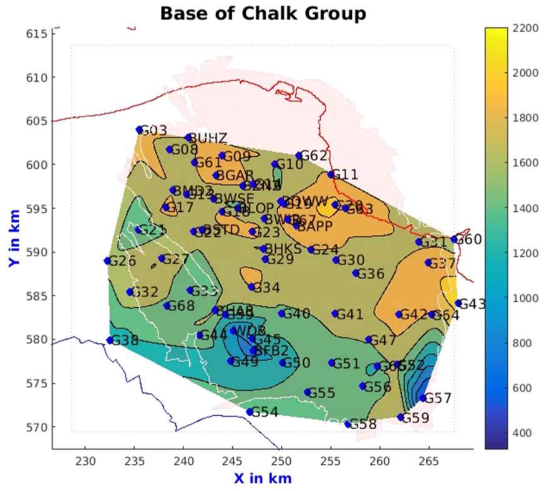

Figure 5 The depth calculated using equation (3) for the base of the Chalk group.

Figures 6 and 7 show comparisons between the depths of the respective interfaces underneath various stations according to the provided velocity model, and the same depths estimated using our method. The shallow part of the provided velocity model is known to be less constrained because the 3D survey used to build it was designed to image the reservoir. A perfect match between the model and our results therefore should therefore not be expected. However, we see a good agreement between the model and our results for the majority of the stations.

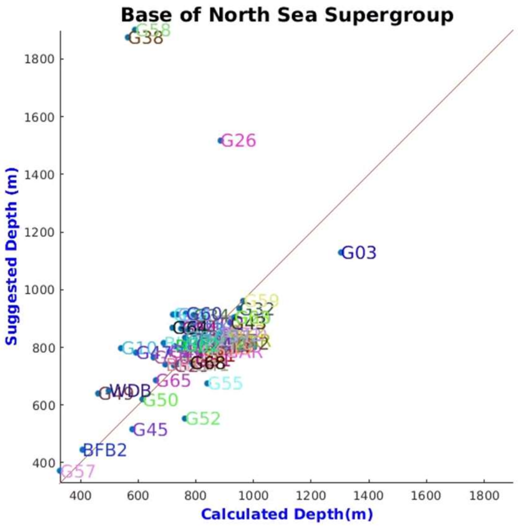

Figure 6 The approximate depth calculated using Equation 3 vs. the depth according to the velocity model for the base of the North Sea supergroup.

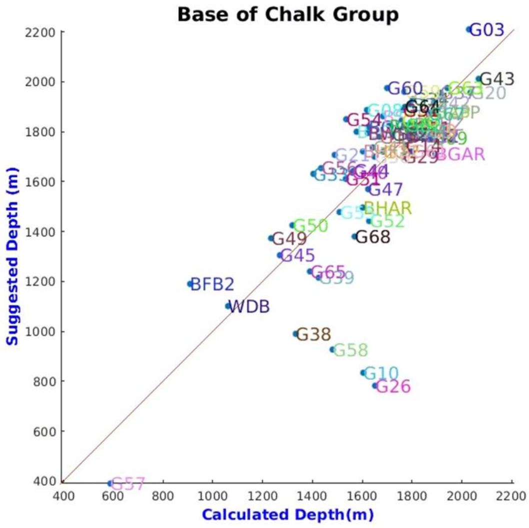

Figure 7 The approximate depth calculated using Equation 3 vs. the depth according to the velocity model for the base of the Chalk group.

CONCLUSIONS AND DISCUSSION

In this paper, we have analyzed induced seismicity data from the Groningen gas field. We have shown that it contains phase conversions from interfaces within the subsurface. Through a combination of finite-difference simulations and kinematic analysis we were able to identify the origin of these conversions.

We also showed that conversions recorded at the surface may be used to image the corresponding structures. Relative abundance of seismicity in the Groningen area allowed us to collect enough data to estimate zero-offset move-outs for direct and converted phases, and then use these move-outs to convert them to the interface depths at different location.

An alternative way to use the time differences would be to assume that the depth to the interface and the P-wave velocity above the interface are known by well logging. Then, one could determine an average S-wave velocity to the interfaces. The S-velocities may be beneficial in ground motion prediction.

ACKNOWLEDGEMENTS

We would like to thank Hua Wang for many fruitful discussions of this project, Saudi Aramco for funding the first author of this manuscript, and Shell Global Solutions International for funding the second author. We would also like to thank NAM providing the model and Sara Minisini for making it available in the right format.